Radboud Repository

Radboud University Nijmegen

PDF hosted at the Radboud Repository of the Radboud University Nijmegen

The following full text is a publisher's version.

For additional information about this publication click this link.
http://hdl.handle.net/2066/24290

Please be advised that this information was generated on 2017-12-05 and may be subject to change.

JOURNAL OF PATHOLOGY, VOL. 178: 268–273 (1996)

MIB1, A PROMISING MARKER FOR THE CLASSIFICATION OF CERVICAL INTRAEPITHELIAL NEOPLASIA

JOHAN BULTEN, JEROEN A. W. M. VAN DER LAAK, JOHANNA H. GEMMINK, MARTIN M. M. PAHLPLATZ, PETER C. M. DE WILDE AND ANTONIUS G. J. M. HANSELAAR

Institute of Pathology, University Hospital Nijmegen, Nijmegen, The Netherlands

SUMMARY

Formalin-fixed and paraffin-embedded tissue specimens of normal and dysplastic cervical epithelia (five CIN1, seven CIN2, five CIN3, and five normal) were assessed by an immunoperoxidase technique, using the monoclonal antibody MIB1, regonizing a formalin-fixation-resistant epitope on the cell proliferation-associated Ki-67 antigen. An image analysis system was used to measure four parameters associated with proliferative activity: the Ki-67 labelling index (LI), the number of Ki-67-positive nuclei per unit length of basement membrane, and the maximum value and 90th percentile of the relative distances of Ki-67-positive nuclei from the basement membrane. All these four proliferation-related parameters were highly correlated with the grade of dysplastic change in the epithelium ($0{\cdot}90<r<0{\cdot}97$, $p<0{\cdot}0001$). The best correlation was found for the 90th percentile of the relative distance and with this parameter all CIN lesions could be correctly classified. The means and standard deviations of the Ki-67 LIs in normal epithelium, CIN1, CIN2, and CIN3 lesions were $0{\cdot}07 \pm 0{\cdot}03$, $0{\cdot}16 \pm 0{\cdot}03$, $0{\cdot}25 \pm 0{\cdot}06$, and $0{\cdot}39 \pm 0{\cdot}06$, respectively. These findings support the theory that CIN involves a progressive dysfunction of the proliferative activity of cervical epithelial cells. Image analysis of MIB1 is a promising alternative method for the objective, reproducible, and reliable classification of dysplastic changes in cervical epithelium.

KEY WORDS—CIN; proliferation; Ki-67; MIB1; monoclonal antibody; immunohistochemistry; quantitative analysis

INTRODUCTION

To classify cervical intraepithelial neoplasia (CIN), pathologists usually rely on histomorphological criteria, such as absence of maturation, nuclear pleomorphism, loss of polarity, and the frequency of mitoses.[1–3] The number of mitoses, the presence of atypical mitotic figures, and the localization of mitoses are particularly used for the histopathological grading of lesions.[4,5] In normal cervical epithelium mitotic figures are rarely encountered; when present, they are confined to the basal layer and are never abnormal. In CIN lesions, the mitotic figures occur more frequently, are found in suprabasal layers of the epithelium, and often have an atypical appearance.[5] These observations suggest that CIN involves a progressive dysfunction of proliferative activity of cervical epithelial cells, whereby proliferating cells are found at progressively higher levels of the epithelium with increasing CIN grades.[6]

Recent semi-quantitative immunohistochemical studies on formalin-fixed and paraffin-embedded archival material, using the monoclonal antibody PC10 which recognizes the proliferating cell nuclear antigen (PCNA), have given further support to this hypothesis.[6,7] A significant positive correlation ($r=0{\cdot}75$, $P<0{\cdot}001$) was found between the CIN grade and a semi-quantitative PCNA grade, based on the highest level at which positive cells were seen in the epithelium.[6] The PCNA grade, however, is not suitable for a reliable classification of CIN lesions and normal cervical epithelium, since only 45 per cent of CIN lesions were correctly classified by this means. The disagreement between the histopathological and PCNA grades might be partly explained by the arbitrary grading system chosen to quantify the proliferative activity and/or by the monoclonal antibody selected to visualize the proliferating cells. The limitations of antibodies that recognize PCNA have been described.[8] In a more recent paper, the same authors have demonstrated that the monoclonal antibody MIB1 is superior to the PC10 monoclonal antibody.[9] MIB1 is a novel monoclonal antibody that recognizes a formalin-fixation-resistant epitope on the cell proliferation-associated Ki-67 antigen.[10,11] Ki-67 antigen is a short-lived non-histone protein, which is expressed during the G1, S, and G2/M phases of the cell cycle, but not in the G0 phase (resting phase).[12,13]

In this study, the MIB1 monoclonal antibody was used immunohistochemically to visualize the proliferating cells within CIN lesions. Application software was developed for an automatic image analysis system which enables a quantitative analysis of the proliferating fraction (Ki-67 labelling index) and the localization of the proliferating cells within the cervical epithelium. The aim of this study was to investigate whether this quantitative analysis of MIB1-positive cells could be of value in the objective classification of CIN lesions.

Addressee for correspondence: J. Bulten, Institute of Pathology, University Hospital Nijmegen, P.O. Box 9101, 6500 HB Nijmegen, The Netherlands.

CCC 0022–3417/96/030268–06
© 1996 by John Wiley & Sons, Ltd.

Received 17 February 1995
Accepted 17 July 1995

MATERIALS AND METHODS

Patients

Formalin-fixed and paraffin-embedded cervical biopsies of 22 patients were used, including five CIN1, seven CIN2, and five CIN3 lesions and five cervical biopsies without histopathological abnormalities. Standard 5 μm thick haematoxylin and eosin-stained sections were used for the grading of the lesions. The cases were selected from the archives of the Department of Pathology, University Hospital Nijmegen. The cervical lesions were graded independently by two pathologists. There was agreement concerning the CIN grade between them in 19 cases (86 per cent). The diagnoses of the pathologists were different in three CIN lesions (14 per cent), but in none of these cases was the difference in the grade of the CIN lesions greater than one. The ultimate grade of CIN was obtained by consensus with a third pathologist. One case was ultimately classified as CIN2 (initially graded as CIN1 and CIN2, respectively), one case as CIN2 (initially graded as CIN2 and CIN3, respectively), and the third case as CIN3 (initially graded as CIN2 and CIN3, respectively).

Immunohistochemistry

Three-micrometer thick paraffin sections were mounted onto polylysine-coated slides and dried overnight at 37°C. Paraffin sections were dewaxed in xylene and rehydrated in a standard series of graded alcohols. Rehydrated slides were placed in a citrate buffer (10 mM, pH 6·0) and heated in a household microwave oven at 90°C for 20 min. After microwave preprocessing, the sections were allowed to cool down to room temperature. Subsequently, the slides were briefly washed with phosphate-buffered saline (PBS, pH 7·4) and an indirect immunoperoxidase technique was used to visualize the Ki-67 antigen, utilizing the following incubation steps. The sections were incubated with the mouse monoclonal antibody MIB1 (Immunotech S.A., France) 1:40 in PBS with 2 per cent normal calf serum overnight at 4°C and subsequently incubated with a rabbit anti-mouse peroxidase (Dakopatts, Denmark) 1:100 in PBS for 60 min at room temperature. The peroxidase-labelled complex was developed with diaminobenzidine (DAB; Vector Laboratories) for 4 min at room temperature and intensified with 5 per cent $CuSO_4$ for 5 min at room temperature. All incubation steps were followed by three washes in PBS of 5 min. Subsequently the slides were slightly counterstained with Mayer's haematoxylin, dehydrated in ethanol and xylene, and finally mounted.

Image Analysis

The slides were analysed using a CCD RGB camera (Sony CA-325P) mounted on top of a light microscope (Axioskop, Zeiss) and attached to a VIDAS^{plus} image analysis system (Kontron Inc., Germany). A × 20 objective with a numerical aperture of 0·5 was used for image acquisition, resulting in pixels with dimensions of 0·39 × 0·41 μm. In each tissue specimen, five to seven fields representative for the CIN lesion were selected and digitized for analysis

For each digitized RGB image, the following procedure was performed. First, curves were drawn interactively by the operator to define the location of the basement membrane and the boundary of the most superficial epithelial layer. Next, the red component of the RGB image was used to define all (MIB1-negative and MIB1-positive) nuclei: a background image was constructed by mean filtering (window size of 25 × 25 pixels) of this image. Then the difference between the red image and the background image was interactively thresholded. On the resulting binary image, a dilation, a filling of holes, and an erosion were successively performed to improve the segmentation result. All resulting objects were individually labelled as nuclei.

To define MIB1-positive nuclei, the blue component of the RGB image was interactively thresholded, as the contrast for the brownish/red positive nuclei was the highest in this image. Then objects with an area less than 10 pixels were removed and every nucleus, defined in the red image, that had any overlap with an object in the resulting image was defined as an MIB1-positive nucleus. The segmentation results were displayed as an overlay on the original RGB image, which could be used by the operator to make corrections interactively for misclassified nuclei or to reprocess the image.

The relative distances of each positive nucleus from the basement membrane and the surface were determined as follows. For each positive nucleus, the distances to the basal and to the superficial curve, respectively, were determined from Euclidean distance maps of images containing these curves.[14] From these distances, the relative distance of a positive nucleus from the basement membrane was calculated; a value of zero indicates that the nucleus was located at the basement membrane and a value of one means that the nucleus was located in the most superficial layer. The number of MIB1-positive nuclei, the total number of nuclei, and the length of the basal layer of the epithelium were also measured in each field. From these quantities several proliferation-associated parameters can be derived and four of these were selected: the fraction of MIB1-positive nuclei (Ki-67 labelling index), the number of MIB1-positive nuclei per unit length of basement membrane, the maximum value of the relative distance, and the 90th percentile of the relative distances of MIB1-positive nuclei from the basement membrane. The latter parameter was chosen because the 90th percentile is more stable than the maximum value of the relative distance, because it is determined on the localization of 90 per cent of the positive nuclei, while the maximum value is based on the position of only one positive nucleus.

Statistics

A commercially available statistical software package (NCSS, Number Cruncher Statistical System) was used to compute the Pearson correlation coefficients (r) and their significance levels (P). The mutual correlations of the different proliferation-associated parameters were considered, as well as the correlations between the grade of cervical epithelial lesions and the proliferation-associated parameters.

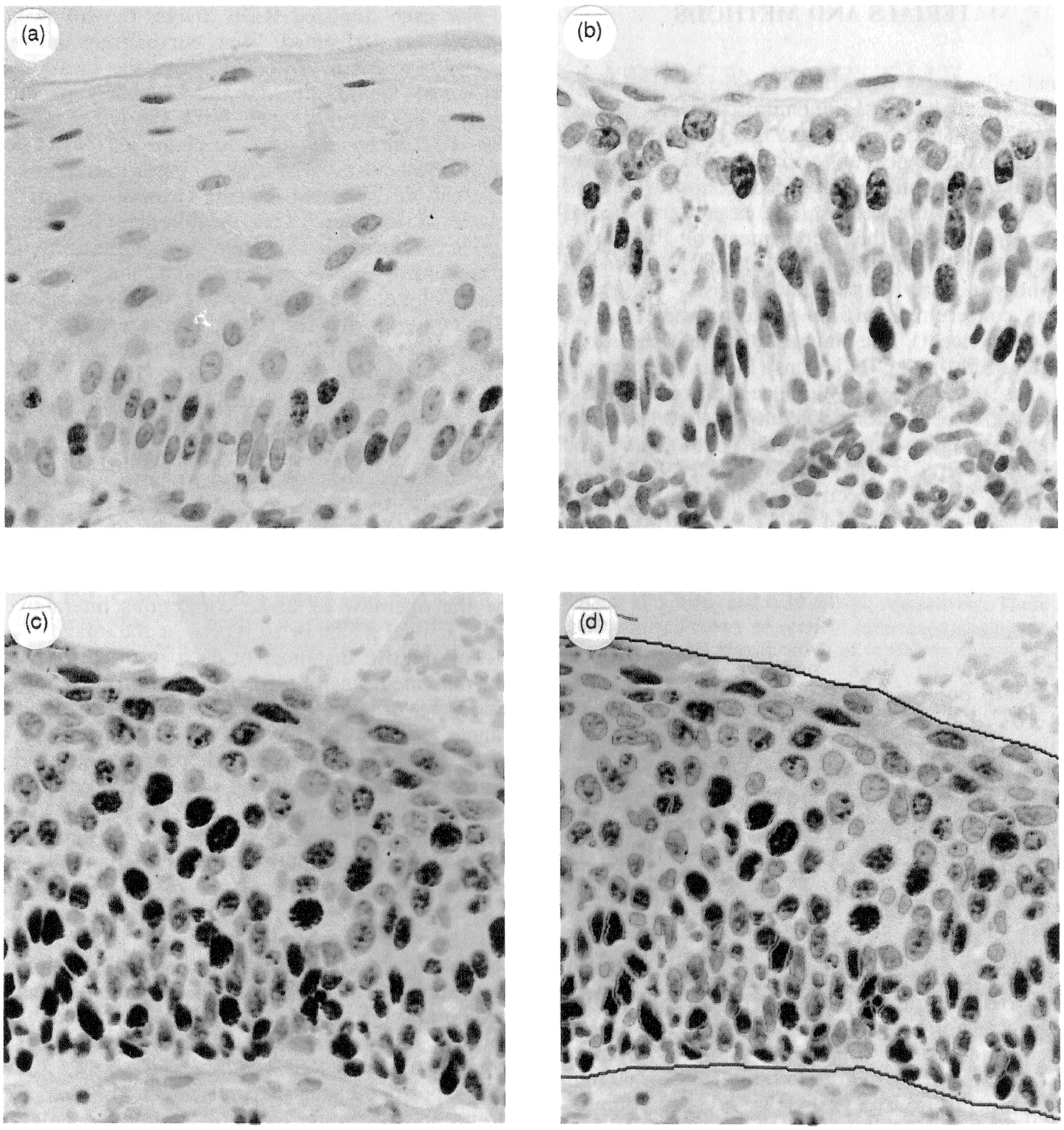

Fig. 1—Indirect immunohistochemical staining of 3 μm paraffin sections of cervical epithelium with MIB1. The peroxidase-labelled immunohistochemical complexes were visualized with diaminobenzidine (DAB) (brown-black). (a) Normal cervical epithelium showing MIB1-positive nuclei exclusively in the basal cell layers. (b) In a CIN3 lesion, MIB1-positive nuclei can be seen throughout the whole thickness of the epithelium. (c) A selected field from a CIN3 lesion with the image analysis system. (d) The results of the RGB segmentation procedure with the VIDAS^{plus} image analysis system in the same CIN3 lesion. Positive nuclei are outlined with a red line and negative nuclei with a green line

NCSS was also used to perform a stepwise linear discriminant analysis to select the best discriminating proliferation parameters and to obtain a linear discriminant classification of normal cervical epithelium, CIN1, CIN2, and CIN3 lesions, based on the selected best discriminating parameter. In the discriminant analysis, equal prior probabilities of 0·25 were chosen, because these prior probabilities are unknown. Choosing equal prior probabilities results in the best compromise between specificity and sensitivity.

RESULTS

The indirect immunoperoxidase staining procedure with MIB1 gave excellent staining results in the Ki-67-expressing nuclei, with hardly any background staining. In normal and squamous metaplastic epithelium, MIB1-positive nuclei were most often found in the basal and parabasal cells. In the CIN lesions, both the fraction of MIB1-stained nuclei and the height of positively stained nuclei increased progressively with the grade of the CIN

Table I—Results of computerized analysis of MIB1 positivity in normal cervical epithelium and CIN1–3

Diagnosis	No. of cases	Fractpos* Mean ± SD	Poslength† Mean ± SD	Reldist90‡ Mean ± SD	Reldist max§ Mean ± SD
Normal cervix	5	0·075 ± 0·031	0·036 ± 0·013	0·150 ± 0·051	0·199 ± 0·088
CIN1	5	0·161 ± 0·026	0·084 ± 0·013	0·324 ± 0·060	0·460 ± 0·096
CIN2	7	0·246 ± 0·060	0·178 ± 0·054	0·510 ± 0·070	0·769 ± 0·067
CIN3	5	0·393 ± 0·060	0·445 ± 0·037	0·846 ± 0·045	0·980 ± 0·016
r value		0·92 ($P<0·0001$)	0·90 ($P<0·0001$)	0·97 ($P<0·0001$)	0·96 ($P<0·0001$)

*Fractpos: fraction of MIB1-positive nuclei (Ki-67 labelling index).
†Poslength: number of positively stained nuclei per unit length of basement membrane.
‡Reldist90: 90th percentile value of the relative distances.
§Reldist max: maximum value of the relative distances of positive nuclei from the basement membrane.
r value=correlation coefficient; *P*=significance level of *r*.

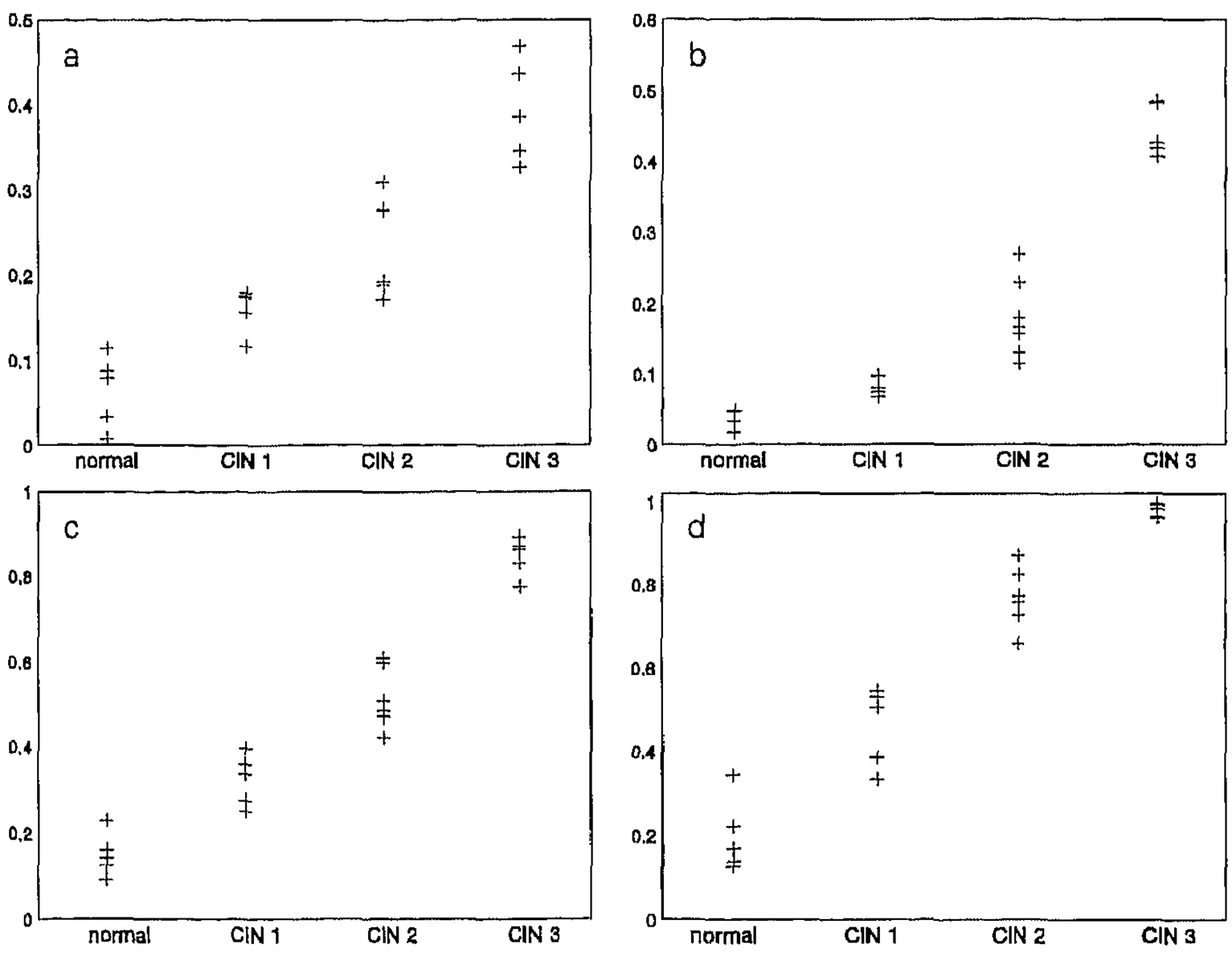

Fig. 2—MIB1 positivity in normal cervical and CIN1–3 epithelia. Relationship between four features of MIB1 positivity and the degree of CIN. (a) Positive fraction (Fractpos) in normal cervical and CIN1–3 epithelia. (b) Number of positive nuclei per unit length of basement membrane (Poslength). (c) 90th percentile value of the relative distances. (d) The maximum value of the relative distances of positive nuclei from the basement membrane

lesion (Figs 1a and 1b). MIB1-stained non-mitotic cells were always found at higher levels than the most superficially located mitotic figures.

Each 'positive–negative' manufactured image was compared by the operator with the corresponding field in the immunostained slide. With the RGB segmentation procedure, it appeared that almost all of the MIB1-positive and MIB1-negative nuclei were correctly recognized by the automatic image analysis system. In general, only minimal interactive interventions were necessary (Figs 1c and 1d).

The mean values and standard deviations of the proliferative-associated parameters for normal cervical epithelium, CIN1, CIN2, and CIN3 lesions are given in Table I. The values of the four proliferation-associated parameters for the individual cases in this study are represented graphically in Figs 2a–2d. Table I and Figs 2a–2d show that the values of all the proliferation-associated parameters increased with increasing grade of the CIN lesion. In CIN3 lesions, the fraction of Ki-67 antigen-expressing cells was approximately 40 per cent and 2·5 times greater than in CIN1 lesions. Fractions of Ki-67-expressing cells exceeding 25 per cent were exclusively found in CIN2 and CIN3 lesions. In normal cervical epithelium, the highest MIB1-positive nuclei were found in the basal third of the epithelium; in CIN1 lesions, the highest MIB1-positive nuclei were noticed in the middle third of the epithelium; and in CIN2 and CIN3 lesions, the highest MIB1-positive nuclei were found in the upper third of the epithelium (Fig. 2d). In

CIN3 lesions, the highest MIB1-positive nuclei were invariably found in the most superficial layers of the epithelium, with a relative distance from the basement membrane greater than 0·95. Correlation analysis revealed that all the proliferation-associated parameters were highly correlated ($r \geq 0{\cdot}90$, $P < 0{\cdot}0001$) with the agreed histomorphological grade of the dysplastic changes in cervical epithelium (Table I). The highest correlations ($r \geq 0{\cdot}96$, $P < 0{\cdot}0001$) were found for the maximum value and the 90th percentile of the relative distances of MIB1-stained nuclei from the basement membrane (Table I). Correlation analysis also disclosed that the proliferation-associated parameters were mutually correlated ($0{\cdot}82 < r < 0{\cdot}99$, $P < 0{\cdot}001$).

In a stepwise linear discriminant analysis, including the four proliferation-associated parameters, the 90th percentile of the relative distances of MIB1-positive nuclei was selected as the best discriminating parameter to classify the cervical epithelium as normal, CIN1, CIN2, or CIN3. Because the proliferation-associated parameters are mutually strongly correlated, only univariate discriminant classifiers were considered. With a univariate discriminant classifier, based on the 90th percentile of the relative distances, all cases were correctly classified. Using the other proliferation parameters in univariate linear discriminant classifiers resulted in some misclassifications; for instance, the classifier based on the maximum value of the relative distances gave rise to one misclassification of a normal case as CIN1 (Fig. 2d).

DISCUSSION

The results of this study have shown that automatic image analysis systems can be used to recognize proliferating and non-proliferating cells in normal and dysplastic cervical epithelium in formalin-fixed and paraffin-embedded archival material, using the monoclonal antibody MIB1. The Ki-67 labelling index, the relative distances of the Ki-67 antigen-expressing nuclei from the basement membrane, and the number of cycling cells per unit length of basement membrane could easily and rapidly be determined and gave detailed numerical information on proliferative intraepithelial abnormalities.

All of our quantitative parameters reflecting the proliferative activity and location of the proliferating cells within the cervical epithelium were highly correlated with the histomorphological grade of the dysplastic changes ($r > 0{\cdot}90$, $P < 0{\cdot}0001$). The highest correlations were found for the maximum value and the 90th percentile of the relative distances of MIB1-positive stained cells from the basement membrane ($r \geq 0{\cdot}96$, $P < 0{\cdot}0001$). Using the latter proliferation parameter in a univariate linear discriminant classifier for grading for dysplastic changes in the cervical epithelium, no discrepancies were found with the histomorphological classifications (normal, CIN1, CIN2, and CIN3).

Our results are in complete agreement with those recently obtained by a semi-quantitative grading system of CIN lesions, based on the highest level at which a mitotic figure was seen in the epithelium.[6] The mitosis grade, ranging from 0 to 3, was highly correlated with the histomorphological grade of the CIN lesion ($r = 0{\cdot}96$, $P < 0{\cdot}001$) and there was a 93 per cent concordance of mitosis graded and histomorphologically graded CIN lesions.[6] In the latter study, PC10, a commercially available monoclonal antibody recognizing the proliferating cell nuclear antigen (PCNA), was also used for immunohistochemical visualization of the proliferating cells in formalin-fixed and paraffin-embedded cervical specimens. PCNA staining was graded in a manner similar to the mitotic grade; grade 0 was assigned if no PCNA staining was detected or if the PCNA-positive nuclei were limited to the basal layer and grades 1, 2, and 3 were assigned when the highest PCNA-positive nuclei fell in the lower, middle, or upper third of the epithelium, respectively.

In comparison with the mitosis grading system, PCNA grading correlated less well with the histomorphological grading of the dysplastic changes ($r = 0{\cdot}75$, $P < 0{\cdot}001$) and concordance between PCNA grade and histomorphological grade was obtained in only 45 per cent (31/68) of the cervical tissue specimens investigated. A plausible explanation for this poor concordance is that the arbitrarily chosen PCNA grading system was not suitable for the classification of CIN lesions. Indeed, if we had used a comparable grading system based on the 'thirds' of the epithelium wherein the highest MIB1-positive nuclei were situated (see Fig. 2d) we also would have found a poor concordance with the histomorphological grades, because all our CIN1 lesions would have been classified as CIN2, all our CIN2 lesions as CIN3, and some of the normal specimens as CIN1.

Shurbaji *et al.*[6] found PCNA grades exceeding the CIN grades in 37 per cent of their cases and in 18 per cent of their cases the PCNA grade was lower than the CIN grade. The latter observation especially could not be well explained by the authors, but possible explanation may be found in their choice of PC10 to visualize cycling cells. The complexities of the use of monoclonal antibodies recognizing PCNA were recently reviewed by McCormick and Hall[8] and the superiority of MIB1 in comparison with PC10 was demonstrated more recently by the same investigators.[9] In the latter study they demonstrated that PC10 stained not only the proliferating cells, but also non-cycling cells and that the fraction of positively stained cells is dependent on the dilution of PC10 used in the immunohistochemical procedure. These shortcomings were not found for the MIB1 monoclonal antibody and it was concluded that MIB1 is superior to PC10 for quantifying proliferative activity. Furthermore, differences and fluctuations in fixation conditions have considerable effects on the immunoreactivity of PC10 which can, for instance, be reduced by prolonged fixation.[15] Recently Casasco *et al.*[16] have demonstrated that the loss of PC10 immunoreactivity in formaldehyde-fixed tissues is progressive and already quantifiable after 3 h fixation. In particular, fixation times of more than 6 h resulted in a considerable reduction of the PC10-positive cell fraction.

In this study we found that all dysplastic changes in cervical epithelium were accompanied by increased proliferative activity, as defined by the Ki-67 labelling index (LI). In CIN2 and CIN3 lesions, the Ki-67 LIs were 25 and 40 per cent, respectively. Such high Ki-67 LIs are most frequently described in rapidly proliferating malignant tumours.[17,18] In many malignant tumours, lower Ki-67 LIs were found than in our present study set of CIN2 and CIN3 lesions.[19–21] In well, moderately, and poorly differentiated squamous cell carcinomas of the cervix, the mean Ki-67 LIs were 22·7, 27·0 and 24·2 per cent, respectively.[21] The Ki-67 LIs found in CIN2 and CIN3 were comparable to or even greater than those found in cases of invasive carcinoma of the cervix. In spite of the high proliferative activity in CIN lesions, it is well known that an invasive squamous cell carcinoma will develop in only a fraction of these.[22] It is likely that the high proliferative activity in CIN is controlled by regulating genes and/or proteins. The control mechanisms preventing progression of CIN to invasive squamous cell carcinoma have to be elucidated in more appropriate and informative studies.

We conclude that our results support the theory that cervical intraepithelial neoplasia involves a progressive dysfunction of the proliferative activity of cervical epithelial cells. As a consequence, the use of MIB1, especially in combination with image analysis, offers a promising alternative method for the objective, reproducible, and reliable classification of dysplastic changes in the cervical epithelium. Finally, the image analysis procedure presented here can also be used to assess differences in the expression of other nuclear proteins involved in cell cycle regulation in the cervical epithelium, such as oncogene and tumour suppressor gene proteins.

ACKNOWLEDGEMENTS

This study was supported by a grant from the National Dutch Cancer Society (KUN-92:34). We thank Diagnostic Products Corporation (DPC), Apeldoorn, for their financial support for the colour photographs.

REFERENCES

1. Anderson MC. Female reproductive system. In: Systemic Pathology. 3rd edn. Edinburgh: Churchill Livingstone, 1991; 93–96.
2. Gompel C, Silverberg SG. Pathology in Gynecology and Obstetrics. 4th edn. Philadelphia: J. B. Lippincott, 1994; 113–115.
3. Kurman RJ. Blaustein's Pathology of the Female Genital Tract. 4th edn. New York: Springer-Verlag, 1994; 244–253.
4. Ehrmann RL. Benign to Malignant Progression in Cervical Squamous Epithelium. New York: Igaka-Shoin, 1994; 36–39.
5. Mourits MJE, Peters WJLM, Hollema H, Burger MPM. Three group metaphase as a morphologic criterion of progressive cervical intraepithelial neoplasia. *Am J Obstet Gynecol* 1992; **167:** 591–595.
6. Shurbaji MS, Brooks SK, Thurmond MS. Proliferating cell nuclear antigen immunoreactivity in cervical intraepithelial neoplasia and benign cervical epithelium. *Am J Clin Pathol* 1993; **100:** 22–26.
7. Mittal KR, Demopoulos RI, Goswami S. Proliferating cell nuclear antigen (cyclin) expression in normal and abnormal cervical squamous epithelia. *Am J Surg Pathol* 1993; **17:** 117–122.
8. McCormick D, Hall PA. The complexities of proliferating cell nuclear antigen. *Histopathology* 1992; **21:** 591–594.
9. McCormick D, Yu C, Hobbs C, Hall PA. The relevance of antibody concentration to the immunohistological quantification of cell proliferation-associated antigens. *Histopathology* 1993; **22:** 543–547.
10. Cattoretti G, Becker MHG, Key G, *et al.* Monoclonal antibodies against recombinant parts of the Ki-67 antigen (MIB1 and MIB3) detect proliferating cells in microwave-processed, formalin-fixed paraffin sections. *J Pathol* 1992; **168:** 357–363.
11. Key G, Becker MHG, Baron B, *et al.* New Ki-67-equivalent murine monoclonal antibodies (MIB1–3) generated against bacterially expressed parts of the Ki-67 cDNA containing three 62 base pair repetitive elements encoding for the Ki-67 epitope. *Lab Invest* 1993; **68:** 629–636.
12. Gerdes J, Schwab U, Lemke H, Stein H. Production of a mouse monoclonal antibody reactive with a human nuclear antigen associated with cell proliferation. *Int J Cancer* 1983; **31:** 13–20.
13. Gerdes J, Lemke H, Baisch H, Wacker HH, Schwab U, Stein H. Cell cycle analysis of a cell proliferation-associated human nuclear antigen defined by the monoclonal antibody Ki-67. *J Immunol* 1984; **133:** 1710–1715.
14. Borgefors G. Distance transformations in digital images. *Comput Vision Graph* 1986; **34:** 344–371.
15. Hall PA, Levison DA, Woods AL, *et al.* Proliferating cell nuclear antigen (PCNA) immunolocalization in paraffin sections: an index of cell proliferation with evidence of deregulated expression in some neoplasms. *J Pathol* 1990; **162:** 285–294.
16. Casasco A, Casasco M, Cornaglia AJ, Danova M, Giordano M, Calligaro A. Tissue fixation for immunohistochemial detection of proliferating cell nuclear antigen with PC10 monoclonal antibody. *Biotech Histochem* 1994; **69:** 112–117.
17. Gerdes J, Dallenbach F, Lennert K. Growth fractions in malignant non-Hodgkin's lymphomas (NHL) as determined *in situ* with the monoclonal antibody Ki-67. *Hematol Oncol* 1984; **2:** 365–371.
18. Kuenen-Boumeester V, Kwast van der THH, Laarhoven van HAJ, Henzen-Logmans SC. Ki-67 staining in histological subtypes of breast carcinoma and fine needle aspiration smears. *J Clin Pathol* 1991; **44:** 208–210.
19. Vollmer E, Roessner A, Gerdes J, *et al.* Improved grading of bone tumors with the monoclonal antibody Ki-67. *J Cancer Res Clin Oncol* 1986; **112:** 281–282.
20. Ooms EHGM, Steenbrugge van GJ, Kwast van der THH, Schröder FH. Application of the monoclonal antibody Ki-67 on prostate biopsies to assess the proliferative cell fraction of human prostatic carcinoma. *J Urol* 1991; **145:** 81–85.
21. Wong FWS. Immunohistochemical detection of proliferating tumor cells in cervical cancer using monoclonal antibody Ki-67. *Gynecol Obstet Invest* 1994; **37:** 123–126.
22. Koss LG. The Papanicolaou test for cervical cancer detection; a triumph and a tragedy. *J Am Med Assoc* 1989; **261:** 737–743.